Copyright © 2005 Tech Science Press SID, vol.1, no.1, pp.49-65, 2005

Criteria for the Assessment of Multiple Site Damage in Ageing Aircraft

P. Horst[1]

Abstract: The paper presents a Monte Carlo Simulation method for the assessment of Multiple Site Damage (MSD) and a subsequent attempt to find a way to interpret intermediate results of the Monte Carlo Simulation with respect to the criticality of scenarios. The basic deterministic part of the model is based on the compounding method, which is used in order to gain an acceptable computational effort. Some examples illustrate features of MSD scenarios and this allows to check an approach for feature detection via Wavelet transforms. This Wavelet transform approach shows some positive results in the interpretation of MSD scenarios.

keyword: Multiple site damage, Monte Carlo Simulation, Feature detection, Wavelets.

1 Introduction

The subject of aging aircraft is established at least since it gained a wider public interest after the Aloha incident in 1988. The special problem treated in this paper is the classical MSD (multiple site damage) and to a certain extent the WFD (widespread fatigue damage) problem.

This problem may be divided into different subproblems, which are not all treated in the same depth in this paper. Some of these problems are:

- the question how multiple site damage occurs
- the question of growth of defects in this case, especially the development of cracks of the same size
- the residual strength problem

The first two questions are mainly treated in this paper, while the third one is not deeply looked at. For this third question many publications are known for some years, see e.g. Newman and Dawicke (1995), Atluri (1986), Nilsson and Hutchinson (1994), Horst (2002).

[1] TU Braunschweig, Germany

The approach used in this paper follows a line, which has been kept since the mid to the end 1990sby a group of European researchers as well as some industrial partners in two European projects, namely the GARTEUR Structures & Materials Action Group SM18 and the EU-funded project SMAAC (Structural Maintenance of Ageing Aircraft). This approach consists primarily in a probabilistic view of the process of the evolution of MSD. This approach tries to circumvent expensive full scale tests or very restrictive damage scenarios, since the MCS will yield less drastical scenarios.

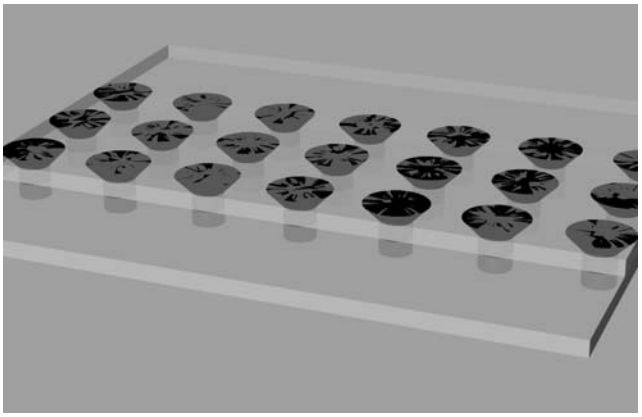

Figure 1 : Typical problem

The special problem treated in this paper is visualized in Fig. 1, it is the classical MSD problem of a riveted longitudinal lap joint in a pressurized fuselage. The stress level is taken as widely constant for at least a set of rivets in a row, and it is taken to act only in circumferential direction.

The general procedure is not limited to this set-up, it is applicable in a much wider sense to other items, which are susceptible to WFD.

The paper tries to summarize the approach used in a number of European companies for the assessment of the susceptibility to WFD as well as by some European researchers today [e.g. Balzano, Beaufils and Santgerma

```
loop over n configurations (scenarios):
        random run for the determination of the initial damage scenario, i.e. definition of damage D(l,0)
        loop over the load cycles i:
                loop over all objects "l":
                        if : object is still in the damage accumulation phase (D(l,i-1) < 1):
                            D(l,i) = D(l,i-1) + dD(l,i)
                        else if : object is an active crack
                            da(l,i) = f(K, ...)   (here:  by means of compounding method)
                            a(l,i) = a(l,i-1) + da(l,i)
                            calculation of plastic zone size
                            check link-up criterion
                check overall residual strength of the structure
        calculation of threshold, interval etc. for the given configuration
calculate statistical values
```

Figure 2 : scheme of the overall model

(1999)]. In addition, it is tried to find an approach to interpret data from these probabilistic analyses with respect to the criticality of designs. This last approach is tried via wavelets as a kind of feature detection.

2 Theoretical background and model

2.1 Overall approach

The overall approach is based on the Monte Carlo Simulation method, which is widely used in different technical and other areas [Melchers (1999)]. This procedure is in a way quite simple, although the actual theoretical and practical background of the method may be complex and also subject to different discussions.

The idea behind this method is to use the scatter in SN-data from small coupon tests to define randomly distributed damage scenarios as initial state for a deterministic calculation. The overall model is shown in figure 2.

The initial damage scenario is defined for a simplified set-up of fatigue critical locations l, this is e.g. the perimeter of a rivet hole etc. It is of course well-known that the actual fatigue initiation location is not always - in an ideal sense - at the perimeter of the hole, but may be located away from the hole at the faying surfaces, see e.g. Schijve (2001). But this point is not essential in this case. What really is needed is a well-defined and statistically sound coupon test of the joint in order to have a well-based fatigue model.

It is quite obvious that many parameters may influence both the fatigue behavior as well as the scatter in this parameter, see e.g. Müller (1995). It is quite clear that especially these parameters may be the key to the occurrence of MSD, if certain features of the fatigue life, i.e. the initiation of cracks, is deteriorated. The information on this point fully relies on basic experimental data. It is not the intention of the model to provide any synthetic fatigue data. It will turn out that the scatter of the fatigue data is really the most relevant parameter for the occurrence of MSD. Therefore, this type of data has to be considered in the preparation of the modelling.

Any additional deteriorating effect, as e.g. corrosion, debonding, badly manufactured rivet rows etc. have to be included into the fatigue data before-hand. They are not explicitly included in the deterministic model.

Surely the question arises, why an approach has been used, which is based on initiation of cracks and a subsequent deterministic crack propagation. The reason mainly lies in the fact that the model for the calculation of the crack growth is surely not prepared to cover extremely small cracks, i.e. cracks with a length lower than a few tenth of a millimeter. Since this would be necessary for an approach, which is based on some "equivalent flaw" type of model, this has not been used. In a way it seems to be of no relevance, whether an equivalent flaw size approach is used, which is based on an insufficient crack growth model or an initiation approach is used, which starts the deterministic modelling at a few tenth of a millimeter crack length.

For the description of the fatigue data and their scatter,

a log-normal distribution has been chosen. This is in a way a compromise. It seems as if the parameters for a log-normal distribution are much more reliably defined by a limited number of fatigue tests than the parameters of a 3-parameter Weibull distribution.

The 3-parameter Weibull distribution would be preferred, since it offers much better results for high numbers of fatigue critical locations, if the size-effect is taken into account, i.e. that a high number of fatigue critical locations are present. The point is that the log-normal distribution has no lower bound and therefore tends to zero, or even negative fatigue life for high numbers of fatigue critical locations, while the Weibull distribution does not show this, since it has a lower limit. This point should be remembered, if really high numbers of fatigue critical locations have to be covered.

In general the damage accumulation law that has been used is the Palmgren-Miner law, i.e. a simple linear accumulation criterion. It is well-known that this law is not flawless, but it provides good data for the more or less constant stress cases, which have been treated in this paper. Although, the basic data on fatigue are taken from (simple coupon) experiments, it is not always simple to find accumulation data for cases, where cracks are already present in the vicinity of the fatigue critical location. Here, a simple model for the influence of higher stresses according to stress concentration α_k-data has been used.

As written in figure 2, each of the n different scenarios is starting with a random distribution of damage at each of the fatigue critical locations. This random process is a "deterministic" random process, which assigns a random value in the interval [0,1] for the value $F(z)$, which is the accumulated probability of failure for each location. The random process is taken from Press, Flannery, Teukolsky and Vetterling (1986). It seems to be reasonable to use a "deterministic" random process, since this allows to repeat runs with the same scenario, if this is needed, e.g. during development of the code or for justification purposes.

There are of course algorithms at hand, which would already provide normally distributed values for z, but these are not used here. One of the well-known approximations for the mapping

$$z = f(F) \tag{1}$$

is used in this code.

It is the general procedure of a Monte Carlo Simulation to use a deterministic model based on the random starting scenario. This is used here. The deterministic model is described in section 2.2.

It may be asked, why a Monte Carlo Simulation has been chosen instead of one of the well-established methods which are often used in structural reliability, like e.g. FORM or SORM etc., see e.g. Melchers (1999), since they usually provide high accuracy with less computational effort.

The reason is that it seems not to be possible to define a conceivable parameter space, which takes into account the relevant data of MSD and on the other hand to put this into one of the methods mentioned above. The Monte Carlo Simulation is much more flexible in this case, although there are some problems arising from the computational effort that is needed for high reliability indices (see section 3.1.2).

2.2 The deterministic model

The type of deterministic model behind this approach is not fixed in any way, apart from the fact that reasonable computational effort is needed in order to achieve a significant number of different simulations, as just stated.

In this paper the set-up depicted in Fig. 1 is idealized in the well-known way of a riveted joint. The three types of loading of the rivet hole, i.e. remote stress, point load and possibly bending may be taken into account. In the present case, a 2D-approach has been used. This is to say that bending has been neglected. This may be a bit astonishing, but results are relatively good, as shown in Horst, Collins, Balzano, Santgerma, Cook, Young, Nilsson, Ottens and ten Hoeve (1997) for different cases, where no thick doubler is used.

Surely other, more sophisticated methods are at hand to do more reliable and more appropriate assessments, as e.g. the finite element method in a 3D version, see e.g. Fawaz and Andersson (2000) for p-elements or others for boundary element approaches. But it is questionable, whether these approaches are able to provide enough data for complex set-ups in a Monte Carlo Simulation. After all, data from such methods are very useful for the check of the 2D results, or may be used for the calculation of individual crack propagation of cracks without interaction (see section 4).

The basic method is the compounding method, which

is well documented in many publications, e.g. Rooke (1977). The basic method is very well described in the ESDU data sheet (1978). The method uses simple single or double crack solutions for the assessment of complex problems, i.e. multiple interactions of cracks and other "boundaries". The basic equation is

$$K_r = K_0 + \sum_{n=1}^{m} (K_n^{'} - K_0) + K_e \tag{2}$$

where K_r is the stress intensity factor of the r-th crack tip, K_n' is the stress intensity factor which occurs from the interaction of crack tip r and boundary n. K_e is an additional factor, which occurs from multiple interaction. This factor is usually not used. It may have a considerable impact, if e.g. a specimen of limited width faces large cracks.

The prime idea of the method is that the stress in the vicinity of the crack tip r is raised by the interaction with the other boundaries and that this is simulated by an additional approach for many boundaries interacting.

This fact has been used to extend the method to partly point loaded rivet holes, since the effect of the stress increase due to other boundaries may also be covered for this case.

The many simple solutions needed for this method have been taken from a set of publications, namely, Rooke and Cartwright (1976), Tada, Paris and Irwin (1973) and Rooke and Tweed (1979). For speed-up reasons these data have been used as interpolated data-sets, equations etc.

What else is needed in this case is a link-up criterion for two adjacent cracks. For crack propagation link-up the criterion proposed by Swift (1992) proved to be useful. This criterion predicts link-up, if the plastic zones in front of the approaching crack tips touch each other.

The Irwin criterion for the assessment of the plastic zone

$$r_p = \frac{K_I^2}{\pi \sigma_y^2} \tag{3}$$

has been used for this purpose, with K_I as the mode I stress intensity factor and σ_Y as yield stress. It is obvious that the criterion largely depends on the definition of the yield stress.

For the crack propagation a simple Forman law has been used, i.e.

$$\frac{da}{dN} = \frac{c_f \Delta K^{n_f}}{(1-R)K_{Ic} - \Delta K} \tag{4}$$

where c_f, n_f and $K_f = K_{Ic}$ are material parameters.

The start crack length of the deterministic calculation has been set to 0.1 mm. This is of course a relatively small size, and it is questionable, whether the model is able to calculate this region reliably, but it surely is not far away from the size, which is well defined.

The relation of the point load from load transfer to the remote stress has been calculated according to the simple models which are given in many publications for the load transfer, as e.g. Niu (1988).

2.3 *Verification of the model*

It is not the intention to repeat the verification of the method by comparison of a complex test result with the method presented here. In fact such a test is quite expensive. Such an expensive test has been performed by Airbus for a longitudinal lap joint within a full scale test, which showed a deteriorated fatigue behavior. The size of the area included a set of frame–bays. Data and the comparison with the compounding method in a MCS have been presented quite some time ago by Horst and Schmidt (1995).

The results have been quite promising. Therefore, it seems to be reasonable to follow this way. What is essential for a good prediction is to have reliable data on the initiation of small cracks. It is not sufficient to use the standard data for the failure of the complete coupon specimen. In order to achieve this, either special inspection methods for quite small cracks are needed during testing, or the failure life data must be used to back-calculate the crack propagation phase and to assess the initiation life by this indirect method.

3 Typical trends in the development of MSD scenarios

Some insight into the evolution of MSD scenarios may be shown by means of a few examples. The basic design of the lap joint is given as follows: two aluminium 2024 T3 sheets, thickness 1.6 mm are riveted by NAS1097 (countersunk) rivets in a three rivet row lap joint. The diameter of the rivets is 4 mm, the rivet pitch is 20mm. It is assumed that the critical row of the lap joint takes a load transfer of 37%.

The remote circumferential stress is taken to 84 MPa, which seems to be a typical stress level for such an item.

The basic material data used in these examples are always the same Forman factors:

$c_f = 2.01 \text{ x } 10^{-8}$

$K_f = 2256 \text{ MPa mm}^{-1/2}$

$n_f = 2.7$

In all cases the critical crack length has been put to 500 mm, which is not completely out of the scope of practical examples (it is more on the smaller side). This means that the critical crack length is not different for all basic examples, since the crack tips are already outside the area of the holes, before the long lead crack becomes critical. The actual critical crack length is not very essential in the scope of this paper, since the few additional load cycles which would be possible for a longer critical crack length are not changing the results considerably.

3.1 Basic influences

The first section deals with some basic influences like the number of fatigue critical rivet locations, the number of required MCS scenarios to be simulated and the basic stochastic parameters like mean life and standard deviation of the fatigue life.

3.1.1 Number of fatigue critical locations

Figure 3 shows the influence of the number of fatigue critical locations on the overall result of a Monte Carlo Simulation.

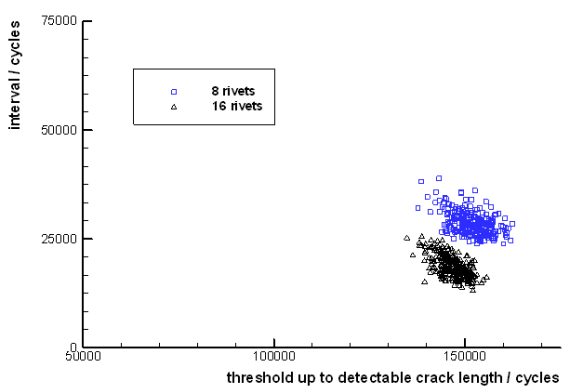

Figure 3 : Influence of the number of fatigue critical locations

The figure uses two output parameters of the Monte Carlo Simulation, which are essential for the determination of the MSD behavior, namely the number of cycles up to the point in time, when the first crack reaches a detectable crack length of 5 mm. This is called "threshold" in this paper. The second parameter is the inspection interval, i.e. the number of cycles between first detectability and the critical state. Both parameters are not affected by any scatter or safety factor.

A number of 250 scenarios per distribution has been used in this case. The mean value for the fatigue life was 115,000 cycles in both cases. The standard deviation is 0.05 in a log-normal scale.

The size effect is clearly visible in this case in two ways: first, the mean value of the distributions visible in figure 3 is decreasing slightly due to the number of possible fatigue critical locations, where the first cracks could start (this is 16 fatigue critical locations in the 8 rivets case and 32 fatigue critical locations in the 16 rivets case). Second, a drop in the interval values.

This set-up with 8 to 16 rivets may be seen as a typical set, which typically occurs in a single frame-bay of a longitudinal lap joint. Normally such a frame-bay is about 500 mm wide, which means more than 16 rivets in a bay, but due to the influence of the frames, the stress in the outer rivets is considerably lower than in the center. Therefore, it is not unrealistic to restrict the focus on this set-up.

From an in-service point of view the outer rivets may be more fatigue critical, although they do not face such high stresses, but they may be more prone to manufacturing problems. This aspect is neglected in this model at this point.

The drop in the threshold values due to the size effect would be much larger, if only a small number of fatigue critical locations is taken into account, but this would not be very interesting with respect to WFD and MSD.

The drop in the interval is mainly explained by the fact that criticality is much earlier reached, if in the case of 16 rivets, a wider area is damaged to a certain extent. This drop may be slighter, if even larger areas are taken into account.

3.1.2 Influence of the number of MSC scenarios

The number of necessary Monte Carlo Simulation scenarios (MSC scenarios) may be assessed by means of

an equation, which has been proposed by Broding, Diederich and Parker (1964)

$$N > \frac{-\ln(1-C)}{p_f} \tag{5}$$

with C as the confidence level and p_f as the required probability of failure.

Figure 4 visualizes this equation for two different confidence levels, namely 0.99 and 0.95.

Supposing that a commercial transport aircraft has a design goal of 40,000 flight hours and a required probability of failure per flight hour of 10^{-9}, the total probability of failure is p_f = 4 x 10^{-5}. The curve for the lower confidence level (0.95) in figure 4 indicates that the required number of scenarios is larger than 74,893 for this case. This is surely a very high number to be simulated even with this very fast and simple simulation method.

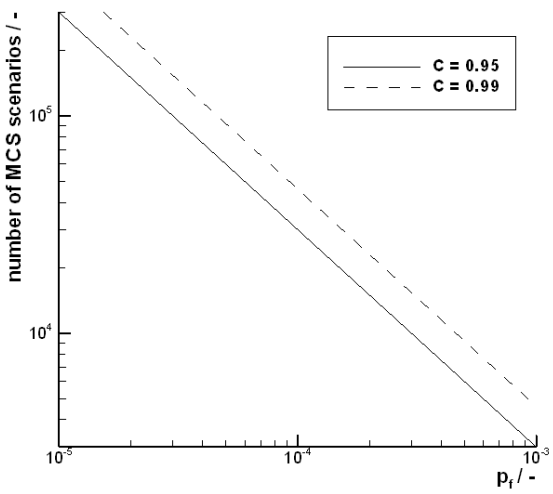

Figure 4 : required number of simulated MSC scenarios

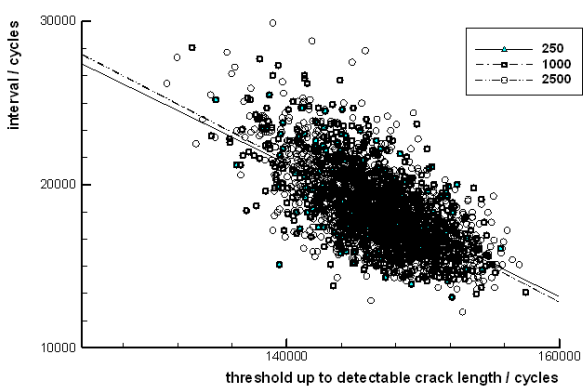

Figure 5 : different numbers of simulations in the case of 16 fatigue critical rivets

Figure 5 shows the results of three different numbers of scenarios in a threshold vs. interval diagram. The results are not very easily to distinguish. It has to be pointed out that the random numbers used in this case are deterministic, i.e. that the first *n* runs of a simulation are the same for each of the cases.

The number of simulation runs in the diagram are: 250, 1000 and 2500. This is of course quite low, in the case of 2500 runs, the probability of failure achieved is approximately $p_f = 10^{-3}$. The computational time used for these 2500 runs has been about 51 min on a 2 GHz PC for the case of 16 fatigue critical rivets in a row.

Figure 5 also includes a linear fit of the data. This linear fit indicates two points. First, the difference between the 1000 and the 2500 scenarios is so small that the two fits are almost not to be distinguished. Second, there is a clear dependency between both output parameters: threshold and interval. This second fact will be better understood in the next sections.

What can be seen in the figure 5 is mainly that with increasing numbers of scenarios simulated, extreme values are slightly increasing. Therefore, it surely is necessary for a reliable assessment to simulate a high number as required, but for the evaluation of the method itself in this paper a lower number must be sufficient.

3.1.3 Extreme values

The values found in figure 5 may partly be interpreted by means of some crack growth data. For this purpose, different results indicated in figure 6 may be used.

These data are both, the minimum and maximum interval as well as the minimum and maximum threshold (again in the sense of fatigue life plus crack growth up to 5 mm detectable crack length). In addition, minimum and maximum life, i.e. the total of all cycles until criticality is given.

Figures 7 and 8 present the crack growth behavior for the case of minimum and maximum interval. All data for the example are exactly like in section 3.1.1.

The number of cycles is given on the ordinate, while the x-direction indicates the x-position, i.e. the horizontal

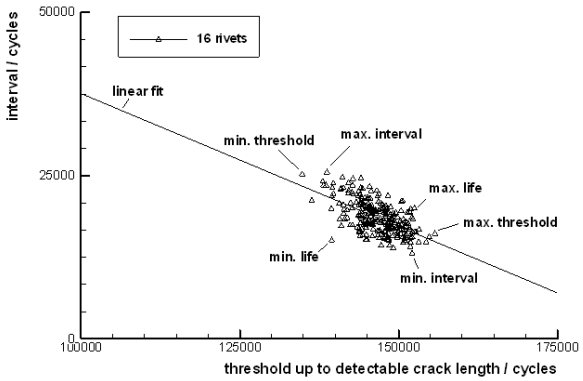

Figure 6 : Extreme values of the MCS

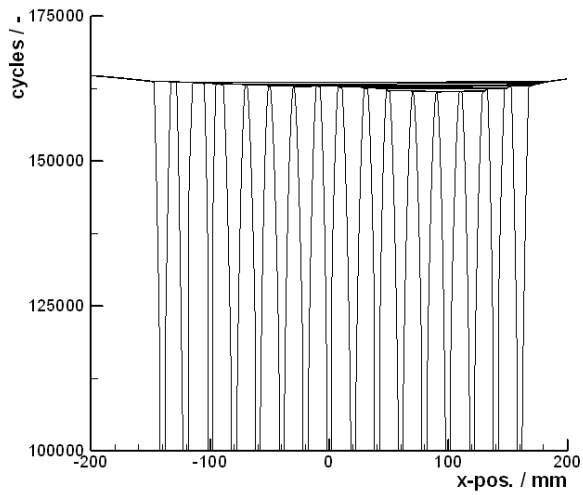

Figure 7 : crack growth for the minimum interval case

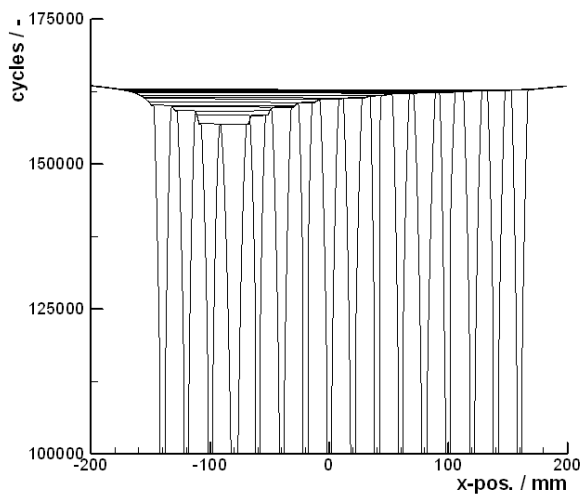

Figure 8 : crack growth for the minimum interval case

position of the perimeter of the rivet hole or the crack tip at this perimeter. In order to keep the information of the two figures in a reasonable scale, the ordinate starts at 100,000 cycles. I.e. that the number of cycles for fatigue and crack growth up to the detectable crack length are not completely covered by the diagrams.

The two figures are showing how the cracks are growing at different holes – at first more or less independently – before at least some are joining to build larger cracks. It is very obvious that this process is quite different in the two cases.

Obviously the minimum interval case produces a set of adjacent cracks of nearly equal size, while in the maximum interval case just a few cracks are growing adjacent to each other. This results in a fairly lower crack growth rate in the final state.

The two figures on the minimum and maximum threshold, 9 and 10 are showing different scenarios, but the basic influences are the same again.

The maximum threshold figure is not meaning too much with respect to the MSD/WFD problem, apart from the fact that it indicates again that scenarios similar to the minimum interval scenario are leading to similar results.

Figure 11 may look a bit strange at first sight, but the final crack scenario results in a critical state, which would join up completely in the next step.

Since all diagrams do not really indicate all three phases of the total life, this is given in Table 1 for the six cases given in the crack growth diagrams.

From all this, the linear dependency of interval and threshold is relatively simple to explain: cases where – due to the size effect – a single crack initiates early, will not have many cracks initiated in the same period. This early, single crack initiation leads to longer crack growth periods, i.e. intervals.

On the other hand, if the first crack initiates lately, the chance that other cracks initiate more or less shortly afterwards is large. This means that a more MSD-like scenario will occur, which results in a much shorter interval.

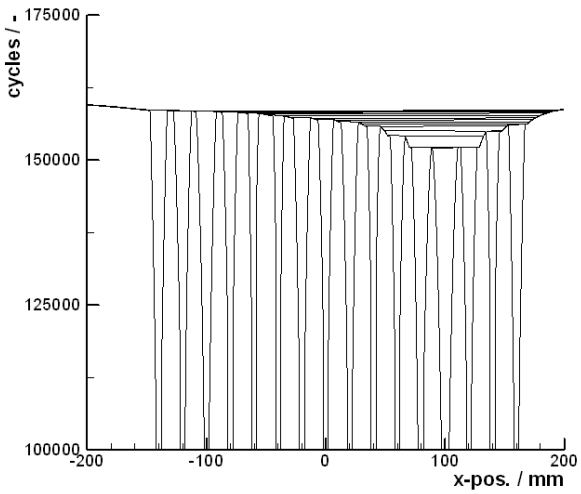

Figure 9 : crack growth for the minimum threshold case

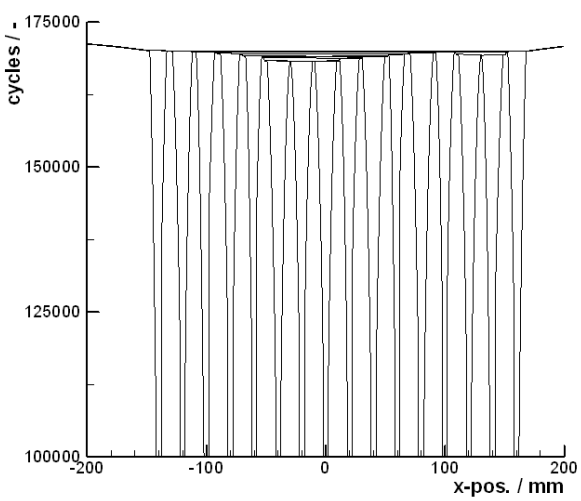

Figure 10 : crack growth for the maximum threshold case

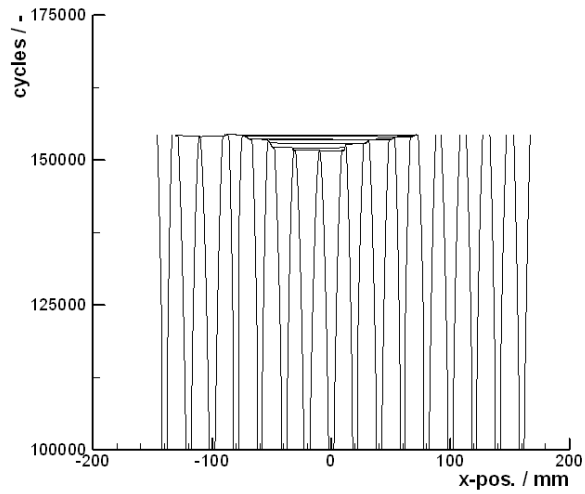

Figure 11 : crack growth for the minimum life case

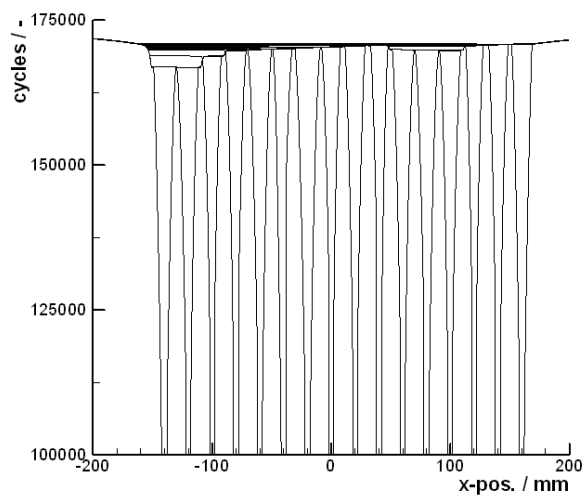

Figure 12 : crack growth for the maximum life case

Table 1 : results for the six extreme values

case	fatigue	crack growth <5 mm	interval
	cycles	cycles	cycles
min. interval	86,315	65,800	13,100
max. interval	77,729	61,000	25,500
min. threshold	78,495	56,300	25,200
max. threshold	97,592	58,100	16,100
min. life	85,059	54,400	15,100
max. life	93,100	59,400	20,000

This aspect will be treated again in more detail in section 4 on feature detection.

3.1.4 Influence of the scatter value of the fatigue data

It is obvious from the statements made in 3.1.3 that both, scatter and mean value of the fatigue data will have a considerable influence on the MSD scenario creation. This point of view is discussed in the present section.

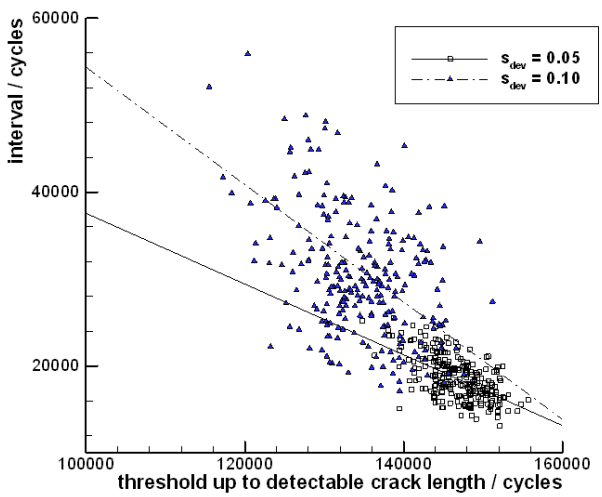

Figure 13 : influence of the standard deviation

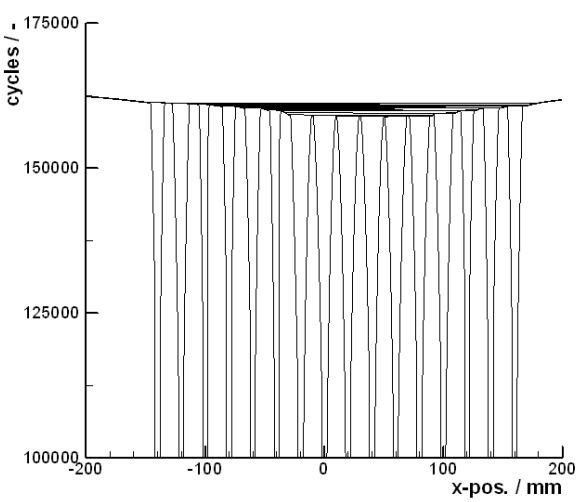

Figure 14 : crack growth for the minimum interval case (s_{dev} = 0.1)

Figure 13 shows the influence of a change in the standard deviation from 0.05, as in the previous examples, to 0.10.

The changes are significant. It is quite obvious that the standard deviation has an impact on both, the threshold as well as the interval. Interpretation of these results is again not too hard to find. Obviously, the higher standard deviation results in a more scattered crack scenario, which in turn results in longer crack growth periods, since less MSD-like scenarios are found.

In addition, since also the threshold up to detectable crack length is influenced, also the linear fit, i.e. the dependency of the two parameters, is changed significantly. This may be seen in figure 14, which is parallel to 7 in all respects, apart from the different standard deviation. Also this is the crack growth curve for the minimum interval case.

Compared with figure 7, figure 14 shows an even more pronounced MSD case of nearly equally sized cracks in the area between $x = [-40, +100]$ *mm*. But in figure 7 the area with nearly as similarly sized cracks is even more widespread, although the outer cracks are not quite as large. This leads to a difference in the interval of

17,100 for s_{dev} = 0.1

13,100 for s_{dev} = 0.05

It can easily be understood that small standard deviations lead to more critical scenarios with respect to MSD/WFD.

3.1.5 Influence of the mean fatigue life

The influence of a decreasing mean fatigue life is shown in figure 15. The basic mean life of 115,000 cycles is compared to a mean life of 80,000 cycles. Both numbers are low for well designed joints, but may occur, if something extra-ordinary happens, as this is the case in MSD/WFD situations.

It can easily be seen in figure 15 that the linear fit lines to the two distributions have almost the same gradient. This means that the dependency between threshold and interval remains the same, even if the threshold value itself drops considerably.

The influences which have been discussed in section 3.1 are surely only a part of all conceivable parameters. Other parameters could be: scattered SN-curves, scattered da/dN-ΔK-curves, scatter in the position of the rivet holes etc.

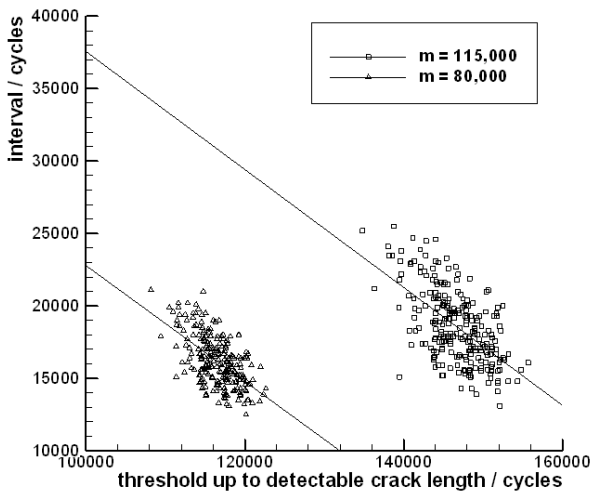

Figure 15 : Influence of the fatigue mean value

Some of theses influencing parameters have been tested in Horst and Schmidt (1995). The paper shows that, although these parameters are interesting for the individual result of a simulation, the overall MCS results are not deeply affected. For this reason, these parameters are left out in this paper.

3.2 More realistic problems

This section is dealing with a more realistic, and also more MSD prone situation. The problem consists of 4 times 16 rivets, which are build in a way that is given in figure 16.

The four parts are slightly separated, as this would be the case for three sets of rivets in adjacent frame-bays, which are all highly loaded compared with the other "outer" rivets.

Figure 17 gives the well-known interval vs. threshold distribution for the two cases of the single 16 rivet set-up and the 4 times 16 rivets set-up.

The results are not extremely different. Primarily the threshold values drop, which can easily be interpreted as a size effect, while the interval values almost remain. This is a very interesting result, because it provides a very simple method to conclude from a few simulated sites to a larger set-up.

This effect is surely linked to the fact that the critical crack length is in the order of magnitude of the frame

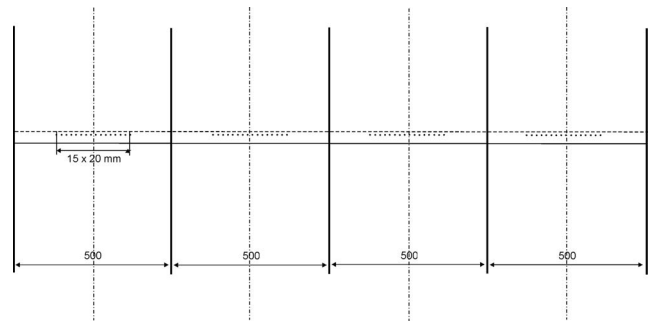

Figure 16 : the more realistic problem of 4 frame-bays (only the critical rivets shown)

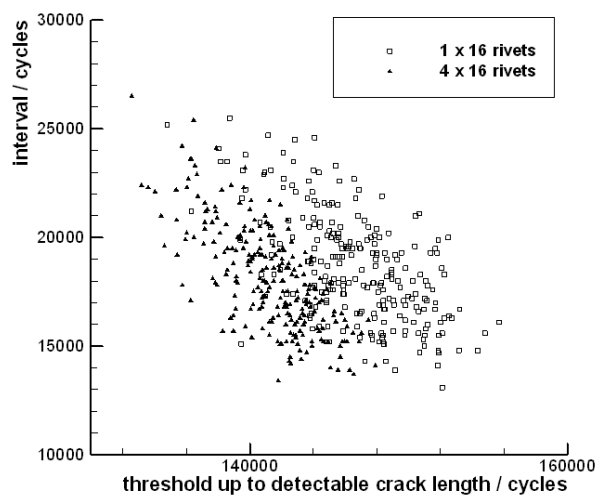

Figure 17 : comparison of the 1 x 16 and the 4 x 16 rivets set-up

spacing, which means that no interaction of the cracks in different frame-bays is needed to reach the residual strength limit.

This effect is also visible in the two crack growth diagrams 18 and 19 for crack growth to minimum and maximum interval.

Both diagrams are only giving a rough impression, since the scale of the x-axis is not allowing to distinguish too many crack growth curves, but the impression of the type of crack growth in both cases is also becoming clear from this overview type of diagram. Only the last few thousand load cycles are shown in order to make the impression more clearly.

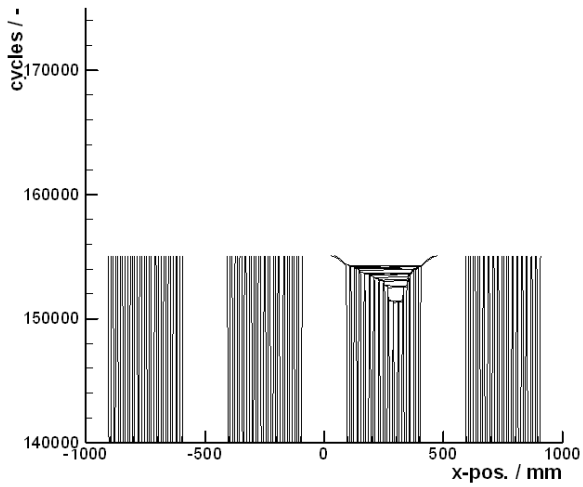

Figure 18 : crack growth up to minimum interval

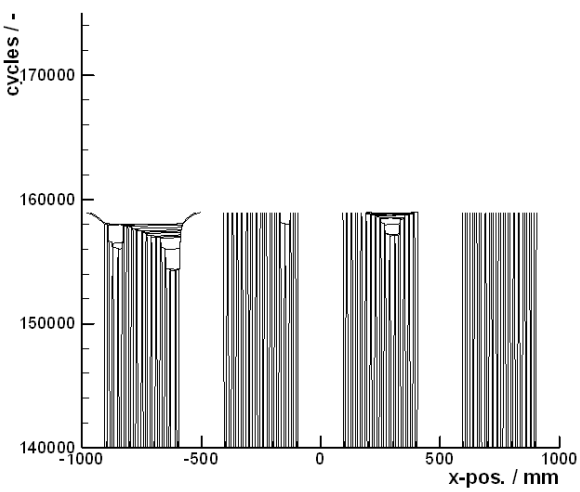

Figure 19 : crak growth up to maximum interval

The computational effort for 250 scenarios of this type of scenario has been approximately 75 min on a 2 GHz PC.

Since figure 17 showed an almost unchanged interval distribution, it would be interesting to try to conclude from single frame-bay scenarios to multiple frame-bay scenarios in the case of the initiation, and therefore the threshold numbers.

The way the size effect may be calculated for the initiation phase is quite simple: the size effect with respect to fatigue may be assessed by means of the equation

$$F^{(n)}(z) = 1 - (1 - F^{(1)}(z))^n \tag{6}$$

where $F^{(1)}$ is the accumulated probability that a single location is facing a fatigue damage at "time" z, while $F^{(n)}$ is the probability that one out of n locations is damaged.

This method can be used in this case. The arithmetic mean and standard deviation for the two cases with 16 and 4 times 16 rivets, i.e. 32 and 128 fatigue critical locations from the MCS are:

Table 2 : fatigue life from calculations via MCS

case	mean value	standard deviation
unit	cycles	cycles
1 x 16	89,778	5,123
4 x 16	84,260	3,827

while the data for both, the complete crack growth as well as the crack growth up to 5 mm crack length are almost not changing.

Table 3 : total crack growth and crack growth up to 5 mm via MCS

case	crack growth		crack growth < 5 mm	
value	mean	standard	mean	standard
unit	cycles	cycles	cycles	cycle
1 x 16	75,439	4,843	56,856	3,911
4 x 16	75,080	4,021	56,947	3,391

The data from table 2 have been used to try to predict the data for the initiation of the 4 x 16 rivets case by using the 1 x 16 rivet data and eqn. 6. From this equation the following relation is found

$$F^{(1)}(z) = 1 - (1 - F^{(32)}(z))^{1/32} \tag{7}$$

$$F^{(128)}(z) = 1 - (1 - F^{(1)}(z))^{128} \tag{8}$$

$$F^{(128)}(z) = 1 - (1 - (1 - (1 - F^{(32)}(z))^{1/32}))^{128} \tag{9}$$

By using equation 9, the data in diagram 20 have been found. A simple normal distribution has been used in this case, a log-normal distribution could even be more appropriate.

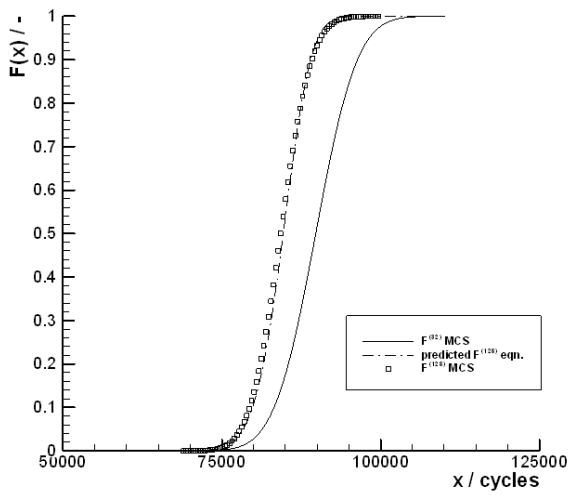

Figure 20 : data from MCS for 1 x 16 and 4 x 16 rivet cases, plus prediction via eqn. 9

By looking at the data, an extremely good agreement between eqn. 9 and the result from the Monte Carlo Simulation is found.

This shows, if the fact that the data in table 3 for crack growth and crack growth until 5 mm crack length are almost the same for both cases is taken into account, that the overall prediction of complex set-ups is possible by using more fundamental example cases. This gives hope that reliable predictions are possible for such complex cases without exhausting computational sources, and to stay in a frame, which is still interesting for the industrial applier.

4 Possibilities of feature detection

It is surely one aim of the work on MSD to judge from data, which are not needing a complete MCS, whether a scenario is likely to result in some sort of multiple site damage, or whether it is far away from this type of damage. Modern ways of feature detection seem a good way to try to achieve this goal.

Two different states of scenarios will be examined in this section for this purpose:

- the initial damage scenario from the random process
- the crack scenario at the point in time, when the first crack reaches 5 mm

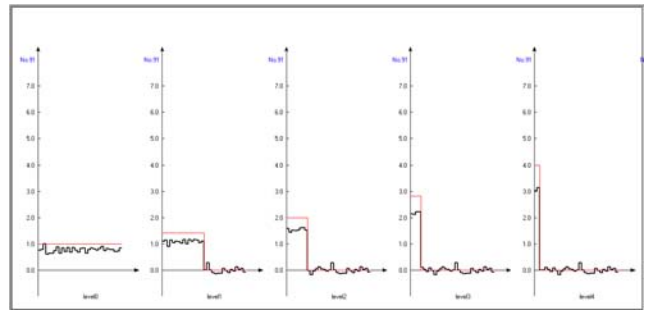

Figure 21 : damage distribution for the minimum interval case, including wavelet transform

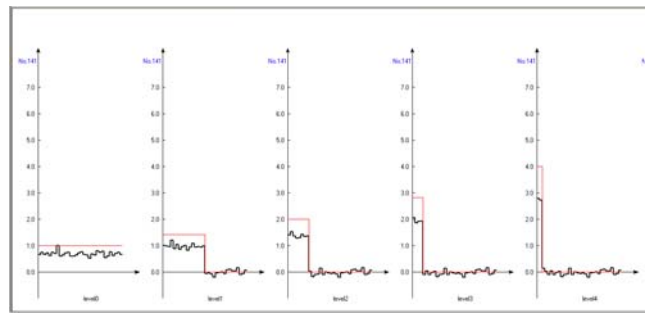

Figure 22 : damage distribution for the maximum interval case, including wavelet transform

Both types seem to be attractive. The first obviously does not need the deterministic calculation, the second only needs the deterministic calculation up to the first crack reaching 5 mm, which means that the cracks (for a rivet pitch of 20 mm) do nearly not interact. This in turn would reduce the computational effort dramatically, it would even allow to use more complex 3D-models for the non-interacting crack growth.

The type of diagram used for this purpose is shortly described by means of figure 21. This figure shows on the left-hand side the distribution of the damage indicated by a normalized number, i.e. damage $D = 1$ indicates the initiation of a crack. The figure shows exactly the situation given by figure 7 for the crack growth of the minimum interval case in the basic example.

Parallel to figure 8, the damage distribution is given in figure 22 for the maximum case.

The diagrams 21 and 22 have to be explained:

The left-hand diagram in both figures shows the distribution of the damage over the 32 fatigue critical locations.

The thinner line marks the case, which would yield ideal MSD, i.e. the same damage everywhere.

The other diagrams are showing a form of a wavelet transform, namely the Haar transform of the distribution. This is a kind of information reduction scheme. A good introduction for this subject is given in Walker (1999).

The Haar transform of the compressed signal works in different levels. This is from left to right, a rising level. The compressed data are getting smaller, while the fluctuations, which are the right "tail" of the graphs are getting longer.

In essence the Haar transform consists in the compression

$$a_m = \frac{f_{2m-1} + f_{2m}}{\sqrt{2}} \tag{10}$$

for the transform and

$$d_m = \frac{f_{2m-1} - f_{2m}}{\sqrt{2}} \tag{11}$$

for the fluctuation, if $\underline{f}$ is the original signal. This process is carried out from one level to the other.

The rising level of the data is based on the fact that this method comes from signal processing, where a reduction of the data requires a higher level, in order to achieve the same energy of the reduced set.

The difference in the damage scenarios as well as in the Haar transforms is not very large, although the two cases are the extremes of the MCS. Therefore, it seems, as if the initial damage scenario is not a very good indication for the MSD-likeness of scenarios.

In figures 24 and 23 the distributions of the crack scenario, i.e. the crack length, of all cracks is shown at the point in time, when the first crack reaches 5 mm. These diagrams are again parallel to the crack growth scenarios in figures 7 and 8.

What may be seen at first sight, is that the distributions (level 0) in the two diagrams are quite different now, and this also seems to be the case for the Haar transforms. In this case the thin line is again the "ideal MSD case", i.e. a 5 mm crack at each fatigue critical location.

It is not possible to show all 250 different scenarios in this way, but there is a certain ranking in the different distributions, which may be used for the assessment of the criticality of a scenario with respect to MSD.

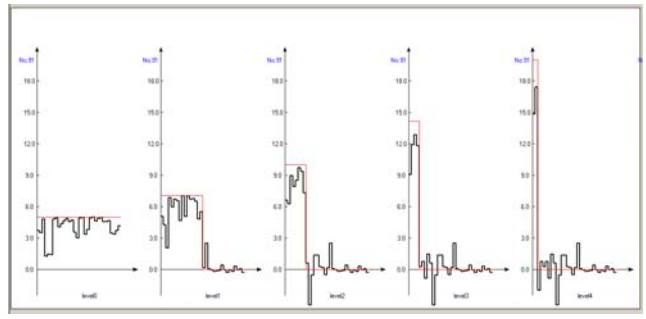

Figure 23 : crack distribution at the point in time, when the first crack reaches 5 mm, minimum interval case, including Haar transform

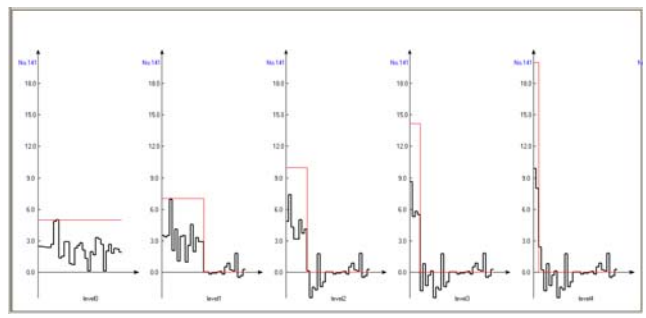

Figure 24 : crack distribution at the point in time, when the first crack reaches 5 mm, maximum interval case, including Haar transform

A small insight in this line may be given by the two diagrams 25 and 26 for the minimum and maximum threshold, as given in figures 9 and 10.

As explained before, in the discussion of figures 9 and 10, the scenarios are near to the ones on the extreme values for the interval, but, due to the negative gradient of the linear fit in figure 6 etc. the minimum and maximum scenarios are exchanged. Gradually, the two distributions are quite near to the extreme values.

What is missing for the assessment of MSD-criticality is something like a "single value"-criterion. One way to try this is the *normalized correlation* between the "ideal distribution" (or a truncated version of this), which is indicated by the thin line and the actual distribution.

The normalized correlation between two discrete distributions $\underline{f}$ and $\underline{g}$ is given by Walker (1999) as

$$\left\langle \underset{\rightarrow}{f} : \underset{\rightarrow}{g} \right\rangle_k = \frac{f_1 g_k + f_2 g_{k+1} + \ldots + f_N g_{k+N-1}}{f_1^2 + f_2^2 + \ldots + f_N^2} \tag{12}$$

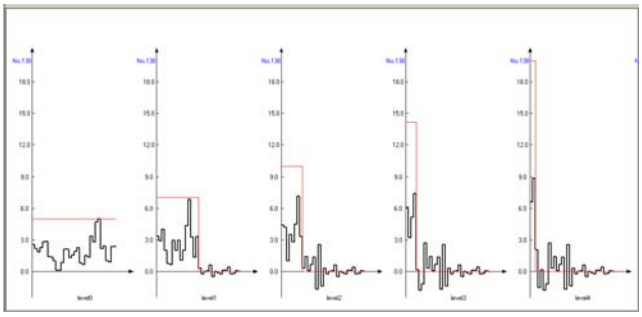

Figure 25 : crack distribution at the point in time, when the first crack reaches 5 mm, minimum threshold case, including Haar transform

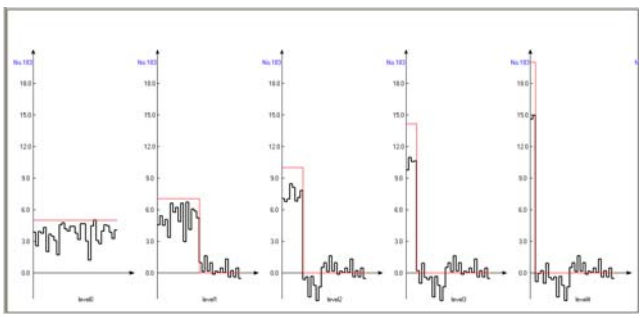

Figure 26 : crack distribution at the point in time, when the first crack reaches 5 mm, maximum threshold case, including Haar transform

where $\underline{f}$ is one distribution ranging from [1, N] and $\underline{g}$ is an other one, which may have an other length and is possibly shifted by a value k.

The "ideal" single value of a normalized correlation would be "1" in this case.

This equation may be used in the determination of a criterion, first for the 1 x 16 rivets case discussed in section 4 up to now, and later on for the 4 x 16 rivets case.

4.1 Correlation in the 1 times 16 rivets case

The results of the normalized correlation of the two "signals", the damage scenario, as it is given in figure 24 for the minimum interval case, and the reference signal of constant crack size 5 mm, has been calculated for all 250 scenarios according to equation 12. The results have been plotted versus the interval, which is e.g. given in figure 6. The result is shown in figure 27.

The correlation has been normalized in two ways, once

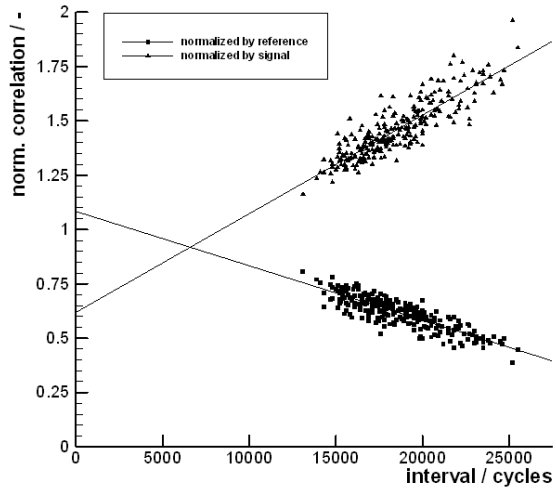

Figure 27 : normalized correlation of the 250 scenarios in the 1 x 16 rivets case vs. interval

by the reference as vector $\underline{f}$ in eqn. 12, and in addition with the actual damage scenario as $\underline{f}$.

It seems to be obvious that none of the two ways of normalization yields more information than the other one. Therefore, it seems to be more appropriate to use the reference as normalizing vector. What is found in the figure 27 is that the correlation obviously offers a good insight into the criticality of a scenario.

One interesting information is that the normalized correlation between any level of the Haar transform and the corresponding Haar transform of the reference results in the same number. This can be used for larger systems if necessary.

The same input as in figure 27 has been used for figure 28, apart from the fact that one additional input has been made. This is the interval for the case of equally sized cracks of 5 mm. The result does not meet the linear fit, but it is in an acceptable distance to the line.

In addition to the data on the crack sizes at the point in time, when the first crack hits 5 mm, the correlation with the initial damage, as it is e.g. shown in figure 21 is given. The optical impression is that the cloud of results is less focussed. Therefore, it seems to be right to rely on the crack scenario and not the damage scenario.

In addition to the 250 scenario cloud, also a 1000 scenario cloud has been added. It might be a bit tricky to

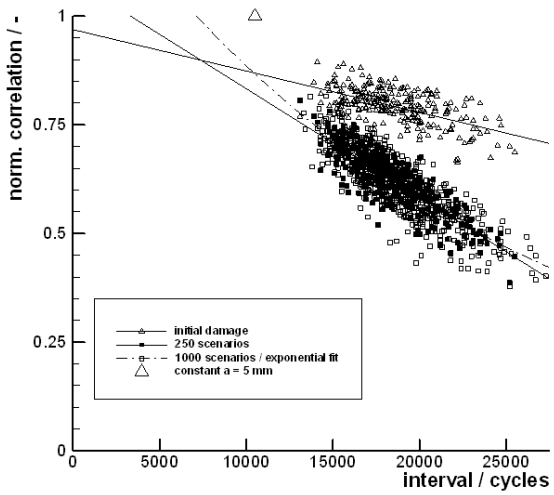

Figure 28 : correlation for the 1 x 16 rivets case, including a constant 5 mm initial scenario

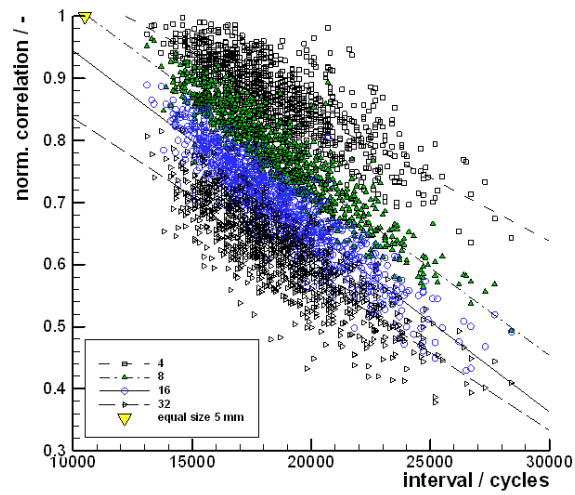

Figure 29 : selective correlation over n fatigue critical locations

keep in mind that this cloud is a bit more scattered. What seems to be essential is that the linear fit is nearly exactly the same as for 250 scenarios.

If a non-linear fit is used, as e.g. an exponential fit in figure 28, the result for the equally sized cracks gets nearer to this line.

There is of course the idea pending that the correlation with the 5 mm "ideal solution" must not be required over the full length of the rivet row. This point is examined in Figure 29. The number of fatigue critical locations which have been used for the correlation analysis are: 4, 8, 16 and 32 (as before). This correlation analysis somehow corresponds to the question how near one of the values in the Haar transform of level 2, 3, 4 and 5 comes to the ideal transform value. It is not exactly the same, since in the Haar transform the blocks of fatigue critical locations are equidistant, while in this case the correlation has been made at steps of one single fatigue critical location.

Surely it is hard to distinguish between the different clouds. But what is visible is the fact that the clouds have different linear fits and are also a bit different in the scatter around the fit. This may be used for the examinations in section 4.2.

A linear correlation coefficient $r < -0.91$ for both, the 8 and the 16 fatigue critical location shows that these criteria via normalized correlation are working quite well.

4.2 Correlation in the 4 times 16 rivets case

The same procedure has now been used for the case of 4 times 16 rivets, i.e. 128 fatigue critical locations. A Haar transform looks a bit more like signal processing in this case. Figure 30 and 31 show the minimum and maximum inspection interval case, as in the preceding sections.

On the left-hand side the original distribution of cracks is shown, while to the right the Haar Transforms are shown.

In this more complicated case, the two original crack distributions do not look so differently, but on the right-hand side level 4 Haar transform is the case, where 16 fatigue locations are indicated by one value. Clearly, the height of this transform is quite different in the two figures. This is a good criterion for MSD-like situations.

In figure 32, this is expressed in another way. Again the normalized correlation (selective over 16 sites) is plotted versus the interval.

The figure supports the impression that this criterion, and this also means the criterion on the level 4 Haar transform, is a good way to assess the MSD-likeness of scenarios. Again the linear correlation coefficient is $r < -0.91$ for this case.

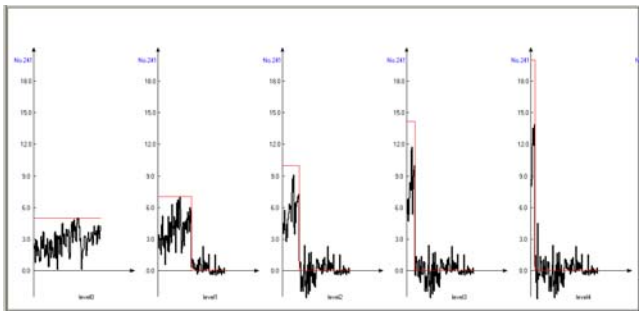

Figure 30 : Haar transform of the 4 x 16 rivet case, minimum inspection

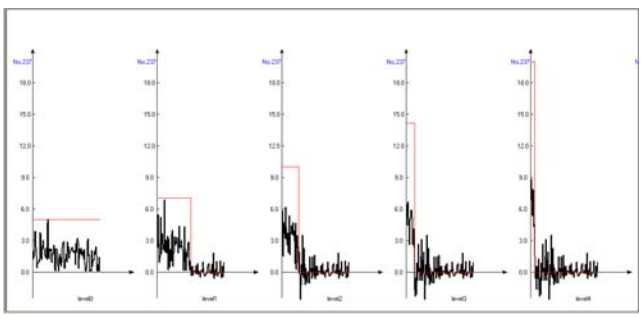

Figure 31 : Haar transform of the 4 x 16 rivet case, maximum inspection

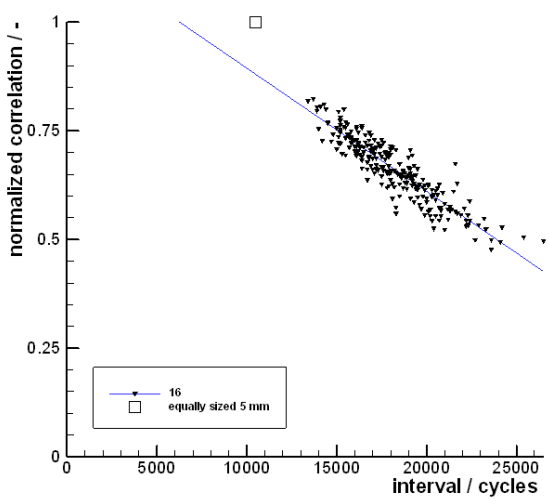

Figure 32 : normalized (selective) correlation over 16 fatigue critical locations for the 4 times 16 rivet case

5 Conclusion

A Monte Carlo Simulation type of approach for the assessment of multiple site damage has been presented. The basic deterministic model behind this approach is a compounding method, which provides a low computational effort method.

Clearly a method is only as good as the reliability of the model used for the prediction. This is especially true for the deterministic model in this case. On the other hand, it is essential to see that the main danger in MSD predictions does not originate from this source. The main source will be false or too optimistic data on fatigue, especially the scatter, since fatigue data seem to be hard to cover for all possible situations which may occur in the life of an aging aircraft.

This argument is even more coming into view, if hazardous situations occur, as e.g. debonding, corrosion etc.

The paper showed that it is possible to predict the behavior of complex set-ups by using more basic and simpler examples.

An attempt has been made to find criteria for the assessment of MSD-criticality, which do not need the complete Monte Carlo Simulation. It has been shown that wavelet transforms of the damage scenario at the point in time, when the first crack reaches detectable crack length, i.e. 5 mm, may serve as a valuable criterion. A selective correlation over 16 fatigue critical locations seems to be of high value.

Appropriate safety margins for practical applications in the order of >3 for the interval and >5 for threshold are not treated here, but they are surely necessary.

Acknowledgement: A part of this paper is based on the work which has been performed in the frame of the EU project SMAAC "Structural Maintenance of Ageing Aircraft".

References

Atluri, S.N. (1986): Energetic Approaches and Path-Independent Integrals in Fracture Mechanics Computational Methods in the Mechanics of Fracture, Chapter 5, S.N. Atluri, Ed., pp. 121-165

Balzano, M., Beaufils, J.-Y. and Santgerma, A. (1999): An Engineering Approach for the Assessment of Widespread Fatigue Damage in Air-

craft Structures, in: Proceedings of "The Second Joint NASA/FAA/DoD Conference on Aging Aircraft", NASA/CP-1999-208982/PART1, pp. 124-131

Broding, W.C., Diederich, F.W. and Parker, P.S. (1964): Structural Optimization and Design Based on a Reliability Design Criterion, J. Spacecraft, Vol. 1, pp 56-61

ESDU data sheet (1978): The Compounding Method of Estimating Stress Intensity Factors for Cracks in Complex Configurations Using Solutions from Simple Configurations, ESDU Item Number 78036

Fawaz, S.A. and Andersson, B. (2000): Accurate Stress Intensity Factor Solutions for Unsymmetric Corner Cracks at a Hole, FFA-Report, Sweden

Horst, P. and Schmidt, H.-J. (1995): A Concept for the Evaluation of MSD Based on Probabilistic Assumptions, in: Widespread Fatigue Damage in Military Aircraft, AGARD-CP-568

Horst, P., Collins, R.A., Balzano, M., Santgerma, A., Cook, R., Young, A., Nilsson, K.F., Ottens, H.H. and ten Hoeve, H.J. (1997): Numerical 'Round Robin' Tests on the Assessment of MSD, Proceedings of the ICAF'97 Congress, Vol. 1, EMAS, West Midlands, pp.

Horst, P. (2002): Multiple Site Damage in Integrally Stiffened Structures, in: Proceedings of the "6th Joint FAA/DoD/NASA Conference on Aging Aircraft", San Francisco, USA

Melchers, R.E. (1999): Structural Reliability – Analysis and Prediction, 2nd edition, Wiley, England

Müller, R.P.G. (1995): An Experimental and Analytical Investigation on the Fatigue Behaviour of Fuselage Riveted Lap Joints, TU Delft

Newman, J.C. and Dawicke, D.S. (1995): Fracture Analysis of Stiffened Panels Under Biaxial Loading with Widespread Cracking, in: Widespread Fatigue Damage in Military Aircraft, AGARD-CP-568

Nilsson, K.F. and Hutchinson, J.W. (1994): Interaction between a Major Crack and Small Crack Damage in Aircraft Sheet Material, Int. J. Solids & Structures, Vol. 31, pp. 2331-2346

Niu, **M.C.Y.** (1988): Airframe Structural Design, Commilit Press Ltd., Hong Kong

Press, W.H., Flannery, B.P., Teukolsky, S.A. and Vetterling, W.T. (1986) : Numerical Recipes – The Art of Scientific Computing -, Cambridge Univerity Press

Rooke, D.P. and Cartwright, D.J. (1976): Compendium of Stress Intensity Factors, HSMO

Rooke, D.P. (1977): Stress Intensity Factors for Cracked Holes in the Presence of Other Boundaries, in: Fracture Mechanics in Engineering Practice", ed. P. Stanley, Applied Science Publishers, pp. 149-163

Rooke, D.P. and Tweed, J. (1979): Opening-Mode Stress Intensity Factors for Two Unequal Cracks at a Hole, RAE Technical Report 79105

Schijve, J. (2001): Fatigue of Structures and Materials, Kluwer Academic Publishers, Dordrecht

Swift, T. (1992): Damage Tolerance Capacity, in: Fatigue of Aircraft Materials – Proceedings of the Specialists' Conference, dedicated to the 65th Birthday of J. Schijve, eds. Beukers, A., deJong, Th.; Sinke, J.; Vlot, A.; Vogelesang, L.B., Delft University Press, pp. 351 - 387

Tada, H., Paris, P. and Irwin, G. (1973): The Stress Analysis Handbook, DelResearch Corp.

Walker, J.S. (1999): Wavelets and their Scientific Applications, Chapman & Hall